Available online at www.sciencedirect.com
SCIENCE DIRECT
Journal of Controlled Release 113 (2006) 15–22
journal of controlled release
www.elsevier.com/locate/jconrel

Using TEM to couple transient protein distribution and release for PLGA microparticles for potential use as vaccine delivery vehicles

Aiying Zhao [a], V.G.J. Rodgers [a,b,*]

[a] The Department of Chemical and Biochemical Engineering, The University of Iowa, Iowa City, IA 52242, USA
[b] Center for Biocatalysis and Bioprocessing, The University of Iowa, Iowa City, IA 52242, USA

Received 28 December 2005; accepted 23 March 2006
Available online 7 April 2006

Abstract

In the development of tunable PLGA microparticles as vaccine delivery vehicles, it is important to understand the drug distribution within the microparticle over time as well as the long-term release of the drug during polymer degradation. This study addresses the transient 3-D drug distribution in PLGA microparticles during in vitro degradation. Specifically, poly (lactide-co-glycolide) (PLGA 75:25) microparticles containing ovalbumin (OVA) as a model protein were fabricated by double-emulsion (w/o/w) method. The microparticles were incubated at 37 °C and 250 rpm in PBS buffer (pH 7.4) over a 100-day period. The in vitro polymer erosion, transient protein distribution profiles and protein release behaviors were investigated. Protein release profiles were determined via spectrophotometry using a BCA assay for the solution. Transmission electron microscopy (TEM) images were obtained for the OVA-loaded microparticles before and during degradation (0 day, 30 days and 60 days), and the corresponding 3-D constructions were developed. From the 3-D constructions, the overall protein distribution of the entire microparticle was vividly reflected. Pixel number analysis of the TEM images was used to quantify transient protein distribution. The transient protein release obtained from the TEM analysis was in good agreement with the BCA analysis. This technique provides an additional tool in helping develop polymer matrices for tunable delivery vehicles in vaccination and other drug delivery scenarios.

Keywords: PLGA; Transmission electron microscopy (TEM); Protein distribution; Biodegradable microparticles; Ovalbumin; Polymer erosion; Polymer degradation; Protein release; Transient release; Time-dependent

1. Introduction

Controlled protein release from biodegradable microparticles has been extensively investigated as potential vehicles for vaccine delivery in the past two decades. Whether for sustained release or pulsatile, the transient protein distribution in the microparticles over long-time, together with polymer degradation, transport characteristics in both bulk erosion and surface erosion, are the primary parameters in determining the efficacy of this methodology [1].

In modeling protein distribution, a uniform protein distribution is usually assumed [2–4]. However, protein distribution profiles may vary among the microparticles for different wall polymer or encapsulated protein due to polymer–protein interactions [5–7]. In addition, various microencapsulation processes involve a number of factors which directly influence the protein encapsulation and the subsequent protein distribution profiles in the microparticles [8–11]. Moreover, although the significance of accurate analysis of protein distribution is apparent, it still remains a challenge to quantify transient protein distribution profiles during the degradation process.

There are, however, a few reports investigating protein distribution in biodegradable microparticles. As some proteins can be fluorescently labeled, confocal laser scanning microscopy (CLSM) was first used to study the detailed protein distribution inside microspheres [3,12,13]. Later, Fourier transform infrared spectroscopy (FTIR) techniques were investigated to determine lysozyme distribution and conformation in a biodegradable polymer matrix [14]. Although both CLSM and FTIR are capable of investigating the internal

* Corresponding author. Current address: Chemical and Environmental Engineering, Center for Bioengineering, University of California, Riverside, A237 Bourns Hall, Riverside, CA 92521, USA. Tel.: +1 951 827 6241; fax: +1 951 827 5696.
E-mail address: vrodgers@engr.ucr.edu (V.G.J. Rodgers).

0168-3659/$ - see front matter © 2006 Elsevier B.V. All rights reserved.
doi:10.1016/j.jconrel.2006.03.018

properties of the microparticles, their resolutions cannot fulfill the requirement of detailed protein distribution in the cross-sections of the microparticles [15,16].

Although, transmission electron microscopy (TEM) is a powerful imaging technique with high resolution for internal structures of materials, it has not been used as often as SEM for the characterization of microparticles [17]. In the area for controlled drug release, the early use of TEM was directed towards the investigations of the outer layer and inner core of double-walled microparticles [18]. Later, Sandor et al. used TEM for pore size analysis of microparticles [19]. Camli et al. investigated the bulk structure of some macroporous latex particles by TEM [20]. Other research teams employed TEM to confirm the shape and size of the microparticles or nanoparticles compared with the images obtained from SEM [21–23]. However, there have been no reports to date on the quantification of protein distribution profiles coupled with transient release.

Compared with other imaging techniques such as CLSM and FTIR, the TEM methods have both advantages and disadvantages [15–17]. The outstanding advantages are that TEM methods can provide the increased resolution and the visualization of the particle ultrastructures. The signal/noise ratio of the protein resolution in the TEM images (comparison of the highlighted areas with the background) is high enough to be incorporated into the montages of the particles without losing any structure information. The montages are the foundation of the resulting 3-D reconstructions. The disadvantages of TEM methods lie in the relatively time-consuming sectioning and staining work. However, as will be shown, TEM can provide a thorough analysis of the protein distribution profiles in the degrading microparticles.

This work addresses the use of TEM as a method to characterize transient protein distribution during long-term microparticle degradation to couple transient protein distribution with delivery. Here transient degradation of PLGA microparticles fabricated by a double-emulsion (w/o/w) method encapsulating ovalbumin (OVA) is investigated. Three-dimensional constructions of transient protein distribution are developed and image analysis is used to quantify protein distribution and release within the microparticles. Finally, protein release rates are compared to the in vitro cumulative protein release over the transient degradation period.

2. Materials and methods

Poly (lactide-co-glycolide) (PLGA) 75:25 (Resomer RG 755, Boehinger Ingelheim, Ingelheim, Germany) were obtained. The average molecular mass was 68 kDa. Ovalbumin (OVA) (Grade V, 44 kDa), bicinchoninic acid (BCA) protein assay, and poly (vinyl alcohol) (PVA) (30–70 kDa) were purchased from Sigma (St. Louis, MO, USA). Methylene chloride (MC) was obtained from Fisher Scientific (Pittsburgh, PA, USA). Eponate 12 resin was obtained from Electron Microscopy Sciences (Hatfield, PA, USA).

2.1. Preparation of microparticles by double-emulsion method

PLGA 75: 25 was used as the microparticle material, MC was used as the organic solvent, PVA was used as the emulsion stabilizer and OVA was the model protein for the degradation and release experiments. Blank microparticles, made by the same procedure, were used as the control.

The microencapsulation procedure was based on the double-emulsion (w/o/w) method. Briefly, 1 g PLGA was dissolved in 25 ml MC; then 1 ml protein solution (30 mg/ml) or DI water was added to 9 ml PLGA solution and sonicated by a sonic dismembrator (Band 1, Model 100, Fisher) for 15–25 s. This w/o emulsion was then poured into 50 ml PVA solutions and sonicated for another 15–25 s with the same sonicator. The double emulsion (w/o/w) was stirred by a Barnant mixer (Band 1, Series 20, IL, USA) for a period of time between 15 and 24 h. The suspension was then centrifuged (Marathon 8 K, centrifuge, Fisher, St. Louis, MO, USA) at 3800 rpm for 15 min. The solids were collected and washed three times with DI water. The microparticles were immersed in liquid nitrogen and then freeze-dried (Freeze Dryer 4.5, Labconco, MO, USA) at −50 °C and 10 μm Hg overnight.

2.2. Determination of protein loading of microparticles

The total protein loading efficiencies of the microparticle were examined by the methods of Coombes et al. [24]. Briefly, an amount of microparticles between 8 and 10 mg was accurately weighed and then redispersed in 3.0 ml of 0.1 M NaOH containing 5% (w/v) SDS. The mixture was incubated overnight in an orbital shaker and then centrifuged. Finally, a BCA protein assay was used to determine the protein concentration in the supernatant. The protein standards were treated in 0.1 M NaOH containing 5% (w/v) SDS. Provided with the measured protein concentration, the total protein loading efficiency (%, w/w) was calculated and expressed as the amount of encapsulated protein relative to the weight of microparticles and as the amount of encapsulated protein relative to the total protein used for microencapsulation. Three samples were assayed for each formulation.

Measurement of surface protein loading was also based on the work of Coombes et al. [24]. Here, 3–4 mg microparticles were accurately weighed and treated with 1 ml of 2% (w/v) SDS solution for 4 h in an orbital shaker at room temperature. Similar to the measurement procedure of total protein loading described above, the samples were centrifuged and the supernatant was analyzed with a BCA assay. The samples were assayed in triplicate. The surface protein loading (%, w/w) was also expressed as the protein percentage in the microparticles and as the protein encapsulated relative to the initial protein weight for microencapsulation.

2.3. Characterization of microparticles by SEM and TEM

The surface properties and size distribution analysis was characterized by scanning electronic microscopy (SEM). The

internal properties, mainly protein distribution and pore occurrence of the microparticles, were examined by TEM (Hitachi H-7000, Tokyo, Japan). The microparticles were treated by a series of procedures before slicing. Microtomy was carried out on a Reichert-Jung Ultracut E microtome (Vienna, Austria) and 80 nm in thickness slices were obtained. Post-staining or post-enhancement was also performed for the best results under TEM.

The following is a brief description of the preparatory procedure for the microparticles with the Eponate 12 resin. The procedure was based on protein fixation and staining [17]. Selected microparticles were encapsulated with 2% w/v agarose, and then fixed by 2.5% glutaraldehyde in 0.1 M Na Cacodylate, pH 7.2. After rinsed with buffer (0.1 M Na Cacodylate, pH 7.2), the sample was stained with 1% OsO_4 (obtained by mixing two parts of 0.2 M NaCacodylate, one part of 4% osmium tetroxide and another one part of 6% potassium ferrocyanide), and then dehydrated with a graded series of acetone (50%, 75%, 95% and 100%), a mixture of 100% acetone and embedding medium (2:1 and 1:2), and pure embedding medium, respectively. Then the sample was embedded in fresh medium and cured in a 50 °C oven for 8 h. Microtomy was carried out and the slices were post-stained with a mixture of uranyl acetate and lead citrate. For the particles labeled with gold conjugates, additional silver enhancement was performed before post staining. During this process, proteins in the microparticles were fixed and stained. The initial protein distribution inside the microparticles remained intact. Finally, the slices were examined using TEM.

TEM imaging was carried out on samples of microparticles representing the initial period, and, subsequently, again every 20 days during the incubation period until only a relatively small quantity of protein could be identified by TEM. For each time period, a complete set of consecutive images of a representative OVA-loaded microparticle before degradation was obtained by series section (as described above). Three complete sets of consecutive images of a representative OVA-loaded microparticle were captured.

2.4. 3-D image construction of the protein-loaded microparticles

The consecutive TEM images for each microparticle were digitally analyzed (Image J, NIH, USA) and brightness and contrast of the images were obtained. Montages for particles were generated in Image J in a similar manner. Finally, the images were reconstructed into 3-D images using Amira 3.0 (Template Graphics Software, Inc., San Diego, CA, USA). The resulting 3-D images visually characterized the protein distribution of the representative particle. Three complete sets of 3-D images of three OVA-loaded microparticles over degradation time respectively (0 day, 30 days and 60 days) were developed. These images were used to analyze transient protein distribution and to analyze mass transfer.

2.5. Pixel analysis of the montages

Pixel analysis of the montages was performed for the protein distribution quantification. The pixel number in protein-distributed areas for each slide of the montage was determined using Image J. The protein distribution profiles were further normalized as a function of the different area for different cross-sections in the microparticle.

2.6. In vitro polymer degradation and protein release

An amount of 10 mg of microparticles (from the same batch used for the initial TEM characterization study) were mixed with 8 ml PBS buffer (pH 7.4) and incubated in an orbital shaker (Model 4520, Thermo Forma, Marietta, OH, USA) under 37 °C and 250 rpm for a period of time until no further protein release was detected. The OVA release profile was measured by BCA assay at various times. The experiment was performed in triplicate and the average values were adopted for the OVA release curve. Simultaneously, a time-dependent BCA calibration curve was developed under the same conditions as the study to correct for spectrophotometric variations due to long-term protein degradation or other signal-altering phenomena. The OVA distribution function obtained from pixel analysis was compared with this OVA release curve measured from experiment.

3. Results and discussions

3.1. Overall microparticle characteristics

Fig. 1 shows a representative SEM image of OVA-loaded microparticles used in this study. As can be seen, under SEM inspection, the microparticles were generally shown to have spherical shape with a smooth surface. Fig. 1 also qualitatively illustrates the particle distribution. Using image analysis

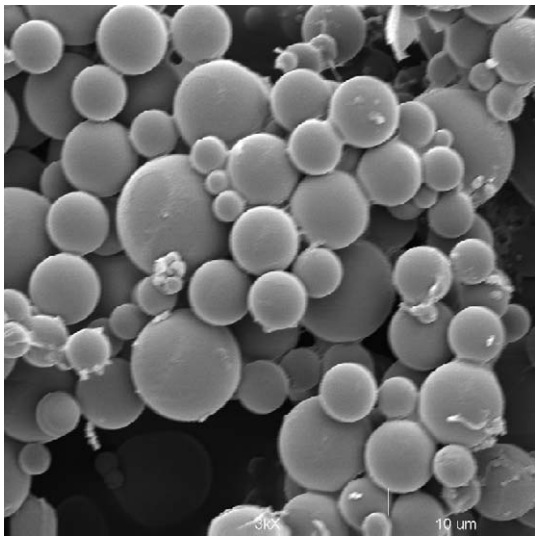

Fig. 1. SEM image of OVA-loaded microparticles constructed from PLGA 75:25 (×1500). The particles were fabricated by double-emulsion method.

software (Image J), the average particle diameter was determined to be 5.1 ± 1.97 μm. The total OVA loading efficiency was determined to be 5.2% w/w (protein/microparticle), which is 60.6% protein loaded/protein used. The surface loading was 3.15% w/w (protein/microparticle) or 60.7% surface protein/total protein loaded. The comparison of total loading and surface loading indicates that a large amount of protein molecules were located on the particle surface or distributed in the large pores connected with the surface. This distribution feature was observed by the protein distribution profiles in the TEM images, which will be discussed in the following sections.

3.2. Protein distribution in the microparticles over time under TEM

Protein fixation was used in the TEM analysis to capture the protein distribution in the microparticle. Protein fixation preserves the protein molecules in as close to the initial state as possible and to allow them to undergo further preparative procedures without altering the position of the proteins. Protein fixation produces coagulation of protein molecules by cross-linking the end groups. This is necessary to prevent their diffusion during further processing [17]. As the glass transition temperature of the wall PLGA 75:25 material ranges from 38 °C to 53 °C during polymer degradation [25], one concern in the processing step in the TEM pretreatment procedure was curing at 50 °C oven for resin polymerization. However, after pretreatment, the particle slices were observed to be generally intact and maintained their original shape as compared to the SEM images (i.e., Fig. 1).

Under TEM examinations, the variation of brightness and contrast reflect the internal characteristics of the cross-sections of microparticles. The polymeric background without the presence of OVA was uniform and moderate in brightness and contrast (Fig. 2). The OVA-distributed areas are characterized by the dark color with a high contrast with the background (Fig. 3A–C). The images are a representation of protein concentration within the center of the microparticle for the specified time of incubation.

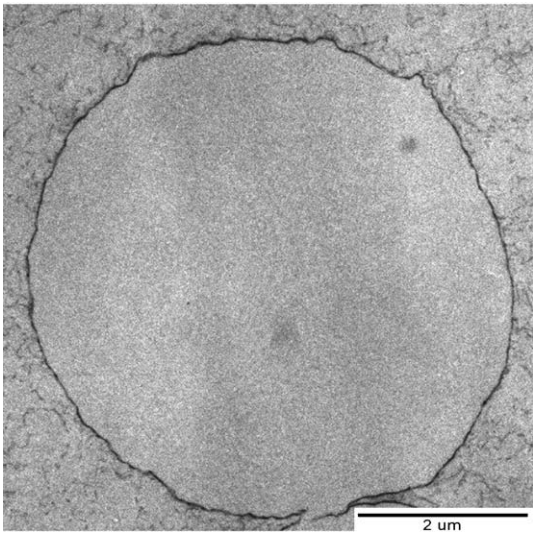

Fig. 2. TEM image of a blank microparticle before degradation. The 80 nm image is taken from a depth of approximately half the diameter of the particle (Control) (×4000).

For each sample, thousands of macroparticles were removed from the incubation mixture and sub-samples were examined using TEM. The images selected are typical representations for the microparticles at the specific time. Although particle size varied, the protein distribution remained similar for the microparticles sampled at the same time (not shown). Thus, this particle size does not notably effect the internal protein distributions. This is consistent with previous researchers who found that the degradation behavior of the polymer matrix was not significantly affected by the particle sizes [26]. It is likely that the encapsulated protein and the wall material (in our case, OVA and PLGA 75:25) are key factors in the development of the protein distribution. In the following discussions, characteristic images were used to show the internal properties for blank microparticles and protein distribution profiles for protein-loaded microparticles before and during polymer degradation, respectively.

The uniform polymeric background of a blank microparticle is also shown in Fig. 2 without any protein or pores present. The TEM images of OVA-loaded microparticles before and during the incubation process demonstrated vivid protein distribution profiles by the highlighted dark-colored areas (Fig. 3A–C). Specifically, these OVA-containing slices showed that the protein-occupying areas were intersected and were visually porous in structure. As all the samples were prepared exactly by the same procedure for TEM investigation, the TEM images can be compared to show the differences or similarities of the internal properties for each sample. By comparison of the blank microparticles (Fig. 2) with the OVA-contained microparticles (Fig. 3A–C), it can be concluded that the TEM staining methods highlighted the presence of protein in the microparticles and therefore provided, at least, a qualitative representation of protein concentration in the microparticles. Later we will show how the pixel number was used to quantify protein concentration.

Protein distribution as a function of incubation time is also illustrated in Fig. 3A–C. During incubation, the OVA-loaded microparticles qualitatively showed a distribution similar to the initial image. As the incubation time increased, the dark color representing the presence of protein continued to fade (Fig. 3B and C). The fading of the dark color over time can be correlated with protein release. Assuming a linear relationship between pixel color intensity and protein concentration, it is hypothesized that OVA release can be estimated from TEM image analysis. This will be shown in the later section of this manuscript.

3.3. Montages of the microparticles before and during degradation

To obtain a 3-D representation of the protein distribution, selected microparticles were sliced as described above into a

series of spatially dependent sections (80 nm thick each) and TEM images were developed for each slice. The series section of a microparticle provided a complete set of consecutive slices

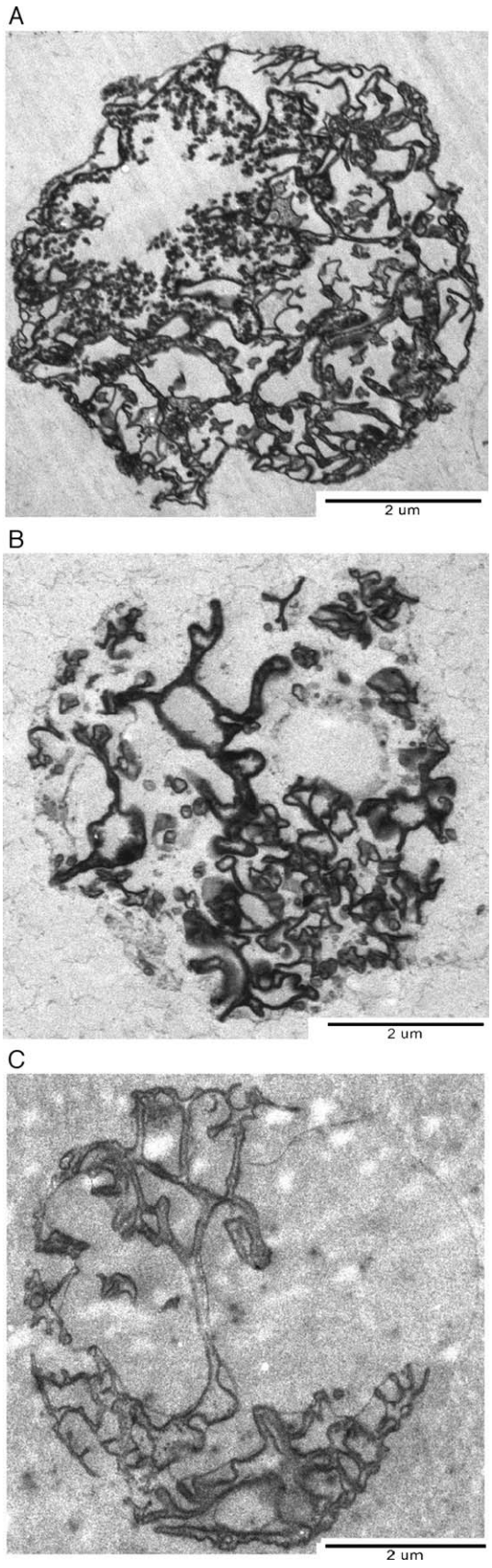

Fig. 3. TEM images of OVA-loaded microparticles during degradation in an in vitro incubation batch process. The samples were first stained by osmium tetroxide, and then post-stained by the mixture of uranyl acetate and lead citrate. The 80 nm image is taken from a depth of approximately half the diameter of the particle. Protein distribution is represented by the dark areas. (×4000) (A) 20 days; (B) 40 days; (C) 60 days.

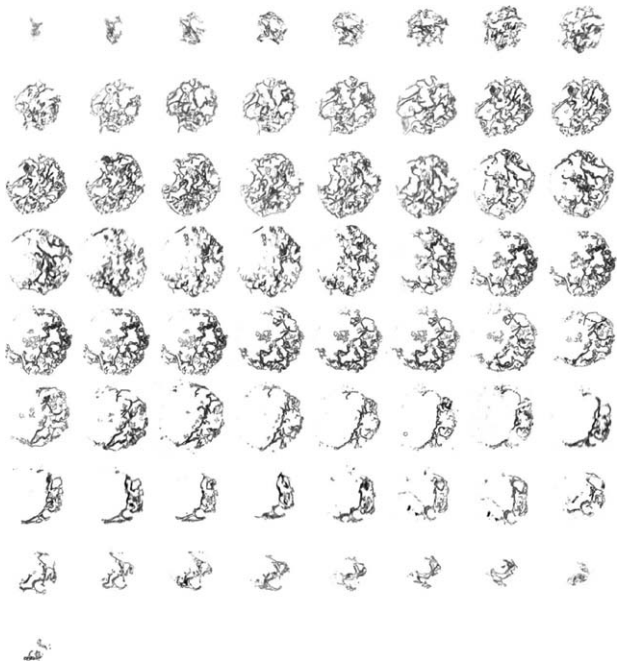

Fig. 4. Illustration of a montage of the protein distribution in a representative OVA-loaded microparticles before degradation. The samples were stained by osmium, and then post-stained by the mixture of uranyl acetate and lead citrate. Each image represents a consecutive 80 nm slice throughout the microparticle (×4000).

of a single particle, which reflected the 3-D protein distribution. Fig. 4 illustrates the montage of 2-D images that are constructed to produce a 3-D protein distribution of OVA encapsulated in PLGA 75:25. In Fig. 4, a total of 65 TEM images were used to construct the 3-D representation of protein distribution for that particular microparticle. This same procedure was used to develop 3-D images of protein distribution in representative microparticles recovered from incubation at 30 and 60 day intervals. In this study, all images were analyzed using the same brightness and contrast. This allows direct comparison of the pixel number analysis for determining the protein concentration profiles.

3.4. The 3-D constructions of the microparticles based on the montages

A 3-D construction of the montages from the 0, 30 and 60 day microparticles during incubation were developed. The 3-D constructions can be rotated to provide visual analysis of the microparticle from all angles. Figs. 5–7 illustrate a fixed image of the 3-D constructions for each of the time periods, 0, 30 and 60 days, respectively. The dark areas represent the presence of the OVA molecules. It should be emphasized that

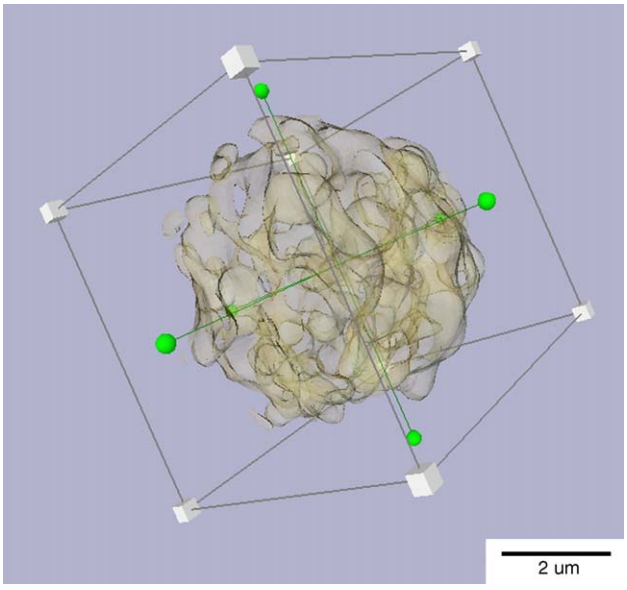

Fig. 5. Image of the 3-D construction of the protein distribution in an OVA-loaded microparticles at 0 days incubation in an in vitro batch process.

PLGA does not produce a signal for this procedure and, thus, the 3-D construction only represents the OVA distribution of the microparticles. From the 3-D construction, the OVA distribution profiles for PLGA 75:25 microparticles during incubation visually remain evenly distributed and the protein concentration demonstrates a gradual decrease from the beginning (Fig. 5) through time course at 30 (Fig. 6) and 60 days (Fig. 7).

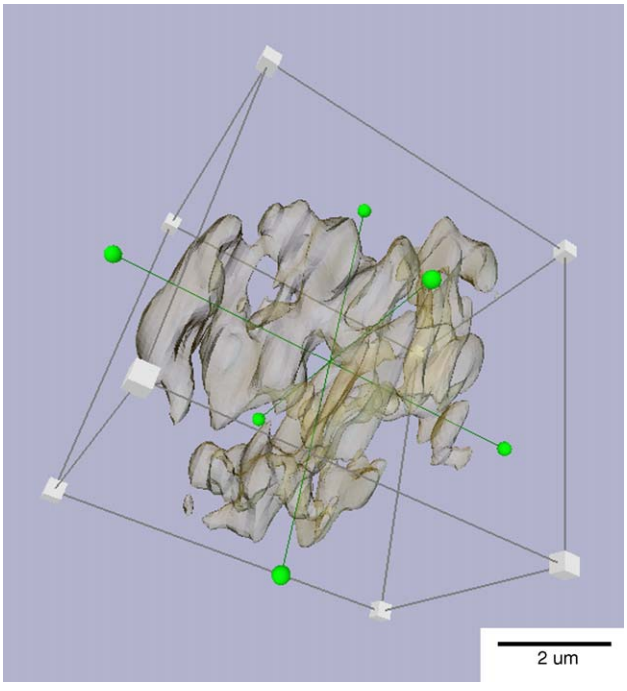

Fig. 6. Image of the 3-D construction of the protein distribution in an OVA-loaded microparticles at 30 days incubation in an in vitro batch process.

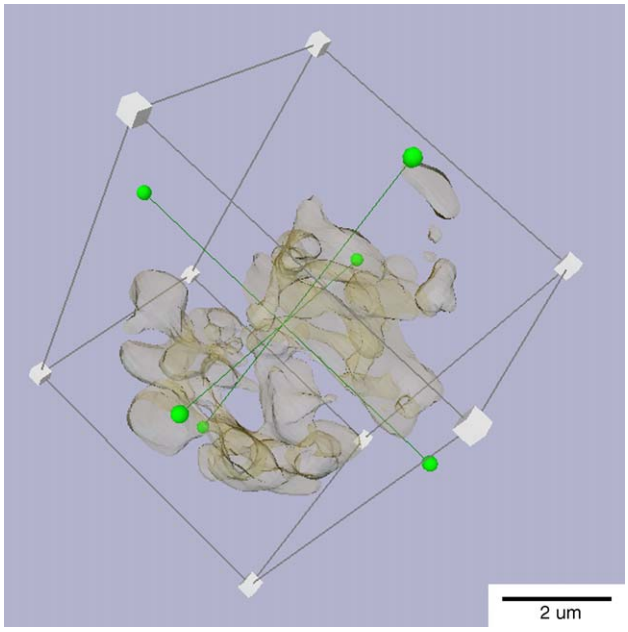

Fig. 7. Image of the 3-D construction of the protein distribution in an OVA-loaded microparticles at 60 days incubation in an in vitro batch process.

3.5. Pixel number as representative of concentration

A more quantitative analysis of protein concentration may be obtained by determining the pixel number of the TEM images. The pixel number, determined by Image J, was assumed to quantitatively represent the protein concentration within each of the TEM images. Fig. 8 is the result of the pixel number analysis from the montage of each particle representing the time course (0, 30 and 60 days) of the incubation period. The total pixel numbers are 110,120, 71,944 and 46,490 for an incubation period of 0, 30 and 60 days, respectively. Thus, about 34.7% of OVA was released in the first 30 days and an additional total release of 24% occurred in the subsequent 30 days. When the

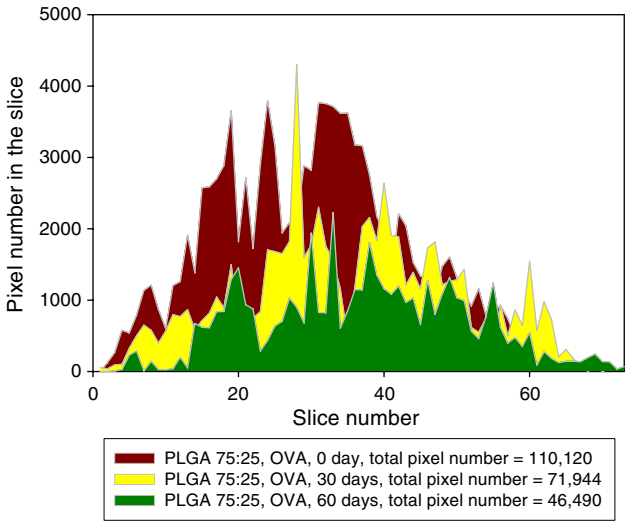

Fig. 8. Pixel number analysis of transient protein distribution and total protein from TEM images for OVA-loaded microparticles over incubation time.

degradation and release proceeded to 60 days, 42% of the initial OVA loading remained in the microparticle.

3.6. Comparison of pixel number mass balance to experimental protein release curves

To verify the significance of the TEM analysis for protein concentration, the total pixel number was converted to a representation of the remaining protein in the microparticle and these results are compared with the BCA protein release data. Recall that the release data is independent of the TEM analysis.

From the BCA analysis, a small release (2.7%) associated with the surface proteins was observed for the initial burst followed by the sustained release from the microparticles over 60 days. At 30 days, 32.3% of the total OVA was released. By the incubation of 60 days, the percent of cumulative OVA release reached 53.9%. It should be noted that a larger burst release corresponding to a high surface protein loading (60.7% in the total loading) was not observed as expected. The possible reason can be attributed to interactions between the polymer wall and the encapsulated protein. Protein adsorption has been realized to be an important factor for protein release from biodegradable microparticles by some other researchers [7,27,28,29]. Recent work by Duncan et al. suggests that the degree of protein solubilisation is the dominant factor for the initial burst [30]. In this research, OVA adsorption to the PLGA 75:25 and OVA aggregation could be the main causes to the release delay.

A comparison of the cumulative OVA release profile determined experimentally during the 70-day incubation using the BCA analysis and that determined from the TEM image analysis is shown in Fig. 9. The results show that the pixel number analysis from the TEM images provided very good agreement with the BCA protein solution method, albeit having a noisier signal. This observation also strengthens the argument that this TEM analysis is representative of cumulative protein distribution within the microparticle. In summary, this TEM analysis has the potential for being a very useful tool for analyzing delivery vehicles.

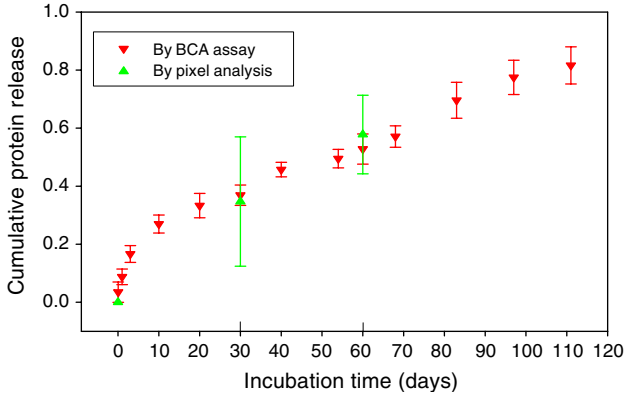

Fig. 9. Comparison of the cumulative OVA release measured by BCA assay of protein in solution with the results obtained from pixel analysis of TEM images.

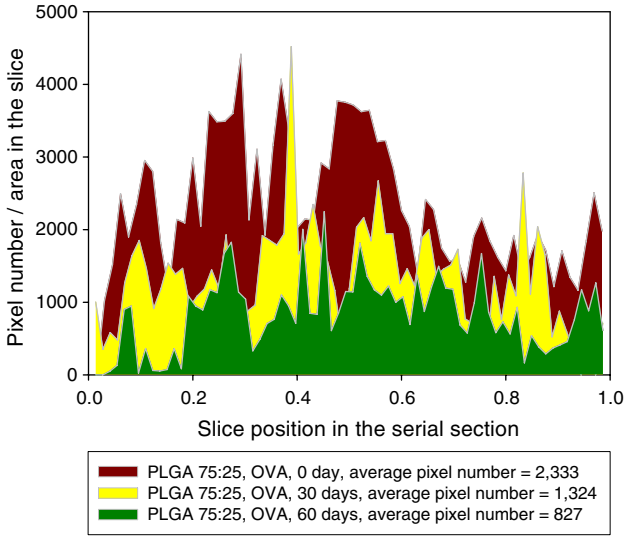

Fig. 10. Pixel number analysis of normalized transient protein concentration from TEM images for OVA-loaded microparticles over incubation time.

3.7. Using pixel number for quantitative analysis of protein concentration distribution

One of the main advantages of the 3-D constructions of protein distribution in the microparticles during transient release is that one can obtain the protein concentration distribution of the microparticle over time. The OVA concentration distribution for microparticle representing the various time periods during incubation were normalized with respect to area and compared to analyze the transient protein concentration distribution. Fig. 10 illustrates the results. The slice numbers were normalized with respect to fraction of microparticle diameter. As can be seen, although significantly noisy, the overall protein distribution within the microparticle remained globally uniform throughout the incubation period. Thus, the TEM image analysis has potential as a valuable tool in monitoring protein concentration in release studies. This method has particular importance when investigating the transport properties of macromolecules in developing tunable polymers for vaccine delivery.

4. Conclusion

A TEM investigation combined with pixel analysis was capable of thoroughly analyzing transient protein distribution of PLGA microparticles before and during in vitro release experiments. The montages of the protein distribution profile in a single microparticle at certain incubation time points were used to develop a 3-D construction of the protein distribution. The montages and 3-D construction suggested a foundation for a more quantitative approach to the analysis of transient protein distribution, protein concentration distribution and release. Pixel analysis of the TEM images was used and found to be in good agreement with the protein release data obtained from solution samples using a BCA assay. This work shows that TEM imaging provides a valuable tool for addressing 3-D

protein distribution in microparticles during release. This has tremendous potential when addressing the development of polymeric materials for sophisticated release characteristics such as those needed for a single-shot vaccine delivery vehicle.

Acknowledgements

The authors would like to thank Jian Qiang Shao for his TEM preparation work and Dr. Kenneth C. Moore for his guidance with the TEM images at Central Research Microscopy Facilities, The University of Iowa.

References

[1] J. Siepmann, A. Göpferich, Mathematical modeling of biodegradable polymeric drug delivery systems, Adv. Drug Deliv. Rev. 48 (2001) 229–247.
[2] W.M. Saltzman, R. Langer, Transport rates of proteins in porous materials with known microgeometry, Biophysics 55 (1989) 163–171.
[3] R.P. Batycky, J. Hanes, R. Langer, D.A. Edwards, A theoretical model of erosion and macromolecular drug release from biodegrading microspheres, J. Pharm. Sci. 86 (1997) 1464–1477.
[4] B. Narasimhan, R. Langer, Zero-order release of micro- and macromolecules from polymeric devices: the role of the burst effect, J. Control. Release 47 (1997) 13–20.
[5] D. Knoll, J. Hermans, Polymer–protein interactions, J. Biol. Chem. 258 (1983) 5710–5715.
[6] D. Blanco, M.J. Alonso, Protein encapsulation and release from poly (lactide-co-glycolide) microspheres: effect of the protein and polymer properties and of the co-encapsulation of surfactants, Eur. J. Pharm. Biopharm. 45 (1998) 285–294.
[7] G. Jiang, B.H. Woo, F. Kang, J. Singh, P.P. Deluca, Assessment of protein release kinetics, stability and protein polymer interaction of lysozyme encapsulated poly(D,L-lactide-co-glycolide) microspheres, J. Control. Release 79 (2002) 137–145.
[8] Y. Yeo, N. Baek, K. Park, Microencapsulation methods for delivery of protein drugs, Biotechnol. Bioprocess Eng. 6 (2001) 213–230.
[9] R.C. Mehta, R. Jeyanthi, S. Calis, B.C. Thanoo, K.W. Burton, P.P. DeLuca, Biodegradable microspheres as depot system for parental delivery of peptide drugs, J. Control. Release 29 (1994) 375–384.
[10] R. Jeyanthi, B.C. Thanoo, R.C. Mehta, P.P. DeLuca, Effect of solvent removal technique on the matrix characteristics of polylactide/glycolide microspheres for peptide delivery, J. Control. Release 38 (1996) 235–244.
[11] Y.Y. Yang, T.S. Chung, X.L. Bai, W.K. Chan, Effect of preparation conditions on morphology and release profiles of biodegradable polymeric microsphere containing protein fabricated by double-emulsion solvent extraction technique, Chem. Eng. Sci. 55 (2000) 2223–2236.
[12] H. Rafati, A.G.A. Coombes, J. Adler, J. Holland, S.S. Davis, Protein-loaded poly(D,L-lactide-co-glycolide) microparticles for oral administration: formulation, structural and release characteristics, J. Control. Release 43 (1997) 89–102.
[13] Y.-Y. Yang, T.-S. Chung, N.P. Ng, Morphology, drug distribution, and in vitro release profiles of biodegradable polymeric microspheres containing protein fabricated by double-emulsion solvent extraction/evaporation method, Biomaterials 22 (2001) 231–241.
[14] M. van de Weert, R. wan 't Hof, J. van der Weerd, R.M.A. Heeren, G. Posthuma, W.E. Hennink, D.J.A. Crommelin, Lysozyme distribution and conformation in a biodegradable polymer matrix as determined by FTIR techniques, J. Control. Release 68 (2000) 31–40.
[15] C. Sheppard, Confocal laser scanning microscopy, Oxford: BIOS Scientific, Springer, New York, 1997.
[16] B.C. Smith, Fundamentals of Fourier Transform Infrared Spectroscopy, CRC Press, Boca Raton, 1996.
[17] J.J. Bozzola, L.D. Russell, Electron Microscopy—Principles and Techniques for Biologists, 2nd Edition, Jones and Bartlett Publishers, Sudbury, Massachusetts, 1999, pp. 20–128.
[18] K.J. Pekarek, J.S. Jacob, E. Mathiowitz, Double-walled polymer microspheres for controlled drug release, Nature 367 (20) (1994) 258–260.
[19] M. Sandor, D. Enscore, P. Weston, E. Mathiowitz, Effect of protein molecular weight on release from micron-sized PLGA microspheres, J. Control. Release 76 (2001) 297–311.
[20] T. Camli, M. Tuncel, S. Senel, A. Tuncel, Functional, uniform, and macroporous latex particles: preparation, electron microscopic characterization, and nonspecific protein adsorption properties, J. Appl. Polym. Sci. 84 (2002) 414–429.
[21] J. Molpeceres, M.R. Aberturas, M. Guzman, Biodegradable nanoparticles as a delivery system for cyclosporine: preparation and characterization, J. Microencapsul 17 (2000) 599–614.
[22] Y.-II Jeong, C.-S. Cho, S.-H. Kim, K.-S. Ko, S.-II Kim, Y.-H. Shim, J.-W. Nah, Preparation of poly (DL-lactide-co-glycolide) nanoparticles without surfactant, J. Appl. Polym. Sci. 80 (2001) 2228–2236.
[23] I.-S. Kim, S.-H. Kim, Evaluation of polymeric nanoparticles composed of cholic acid and methoxy poly (ethylene glycol), Int. J. Pharm. 226 (2001) 23–29.
[24] A.G.A. Coombes, E.C. Lavelle, P.G. Jenkins, S.S. Davis, Single dose polymeric microparticle-based vaccines: the influence of formulation conditions on the magnitude and duration of the immune response to a protein antigen, Vaccine 14 (1996) 1429–1438.
[25] R.E. Eliaz, J. Kost, Characterization of a polymeric PLGA-injectable implant delivery system for the controlled release of proteins, J. Biomed. Mater. Res. 50 (2000) 388–396.
[26] J. Siepmann, N. Faisant, J. Akiki, J. Richard, J.P. Benoit, Effect of the size of biodegradable microparticles on drug release: experiment and theory, J. Control. Release 96 (2004) 123–134.
[27] G. Crotts, T.G. Park, Stability and release of bovine serum albumin encapsulated with poly (D,L-lactide-co glycolide) microparticles, J. Control. Release 44 (1997) 123–134.
[28] G. Crotts, H. Sah, T.G. Park, Adsorption determines in vitro protein release rate from biodegradable microspheres: quantitative analysis of surface area during degradation, J. Control. Release 47 (1997) 101–111.
[29] J.-Y. Yoon, H.-Y. Park, J.-H. Kim, W.-S. Kim, Adsorption of BSA on highly carboxylated microspheres—quantitative effects of surface functional groups and interaction forces, J. Colloid Interface Sci. 177 (1996) 613–620.
[30] G. Duncan, T.J. Jess, F. Mohamed, N.C. Price, S.M. Kelly, C.F. van der Walle, The influence of protein solubilisation, conformation and size on the burst release from poly(lactide-co-glycolide) microspheres, J. Control. Release 110 (2005) 34–48.